Nonlinear Absorption Properties in Novel Gold Nanostructured Topologies

R. West, Y. Wang, and T. Goodson III*

Department of Chemistry, Wayne State University, Detroit, Michigan 48202

Received: December 18, 2002

The nonlinear optical (NLO) properties of different gold metal nanoparticle geometries are reported. The results of nonlinear absorption measurements (as well as optical limiting effects) of both gold nanorods and nanospheres are provided. Gold dendrimer metal nanocomposites were synthesized by first using an amine terminated poly(amidoamine) (PAMAM) dendrimer and later a dansyl chromophore functionalized (PAMAM) dendrimer. The characterization of the nonlinear optical effects in both systems is provided. Another dendrimer morphology containing hydroxy terminated PAMAM G5 was also used as a template to stabilize the gold nanoparticles. These results show that the NLO properties of gold nanoparticles not only depend on the geometry of the metal nanoparticles, but also on the templates used to form the nanocomposites.

I. Introduction

The emergence of nanostructured materials in several research areas has resulted in the creation of novel molecular architectures, which are used for many applications. There have been advances in many organic nanostructured materials including the fabrication of polymers,[1] rotaxanes,[2] oligomers,[3] and dendrimers.[4] There have also been developments in inorganic systems such as metal nanoparticles,[5] semiconducting nanoparticles,[6] and quantum dots.[7] A natural evolution of this work leads to the creation of nonlinear optical (NLO) hybrid nanomaterials (containing both organic and inorganic components) with different metal geometries. This includes the fabrication of dendrimer−metal nanocomposites.[8−12] Also there have been advances in the discovery of new optical limiters, such as metal and semiconductor nanoparticles and other nano-structured materials.[13] However, the understanding of the optical properties, in particular, the nonlinear absorption effects, exhibited by different geometries of gold nanoparticles, is still in an early developmental stage.

Recently, the study of optical excitations in metal nanoparticles has attracted great attention, as the details of optical excitations in metal nanoparticles are expected to be different from those in the bulk. For example, investigations of strong enhancement of emission in gold nanorods near the surface plasmon resonance (SPR) has attracted great attention.[11,14] The strong absorption, scattering, and considerable local-field enhancement occurring at the particle's surface plasmon resonance results in a large optical polarization associated with the collective electron oscillations.[15] Because of this, there are many interesting optical properties of metal nanoparticles that give immense enthusiasm for their use in applications such as sensor protection, medicine, and nanoprobes.[16] However, less has been done to characterize the NLO properties of metal nanoparticles with different geometries.

Investigations of plasmon damping in gold nanorods have revealed large local-field enhancement factors and relatively high scattering efficiencies.[17] However, the most significant advances toward understanding the NLO properties of metal nanostructured materials have been through nonlinear transmission measurements.[18−20] Measurements of two-photon absorption (TPA) have already shown that metal nanoparticles excited close to their SPR illustrate very large TPA coefficients.[21] These properties are so impressive that new applications in two-photon fluorescence imaging and nanopattering, have already been demonstrated in the literature.[22,16] Because of their good optical limiting properties gold and silver nanoparticle materials may have applications in nanosensor and eye protection.[13,18,19a,20,23] Certainly, studies that compare the optical properties of these nanomaterials as a function of metal geometry and templating topology are of great use for the development future applications..

In this manuscript, we report the NLO properties of several different metal nanostructured materials including gold nanorods, nanospheres, and dendrimer−gold nanocomposites. The complete synthesis of four different dendrimer−metal nanocomposites is reported. Results of time-resolved fluorescence and fluorescence quenching measurements are provided to analyze the interactions among the dansyl chromophores attached to dendrimer as well as the dansyl units interacting with the gold nanoparticles. A comparison of all of the systems suggests that the nonlinear transmission (NLT) effect of these nanomaterials depends on the geometry of metal, as well as the templates used to form the nanocomposites.

II. Experimental Section

A. Fabrication of Gold Nanospheres and Gold Nanorods. The fabrication of the gold nanorods and spheres used in this study was carried out by a procedure reported in the literature.[11,14a] An electrochemical method was used to produce gold nanorods of different aspect ratios (5.0 used in this study), and a centrifuge separation procedure was applied to separate the distribution of rod lengths.[14a] To make a good comparison of the NLO effects in different metal systems, the absorption of the transverse (at approximately 520 nm) resonance was used as a measure of the optical density of the rods and spheres in aqueous solution.

B. Fabrication of Dendrimer−Gold Nanocomposites. The fabrication of dendrimer−gold nanocomposites was carried out using three different methods. The PAMAM dendrimer can act as either an organic stabilizer or as a scaffolding agent for the gold nanoparticles.[7−9,25] The fabrication of dendrimer−gold

* To whom correspondence should be addressed. E-mail: tgoodson@chem.wayne.edu.

10.1021/jp027762w CCC: $25.00
Published on Web 03/20/2003

nanocomposites was performed by use of different terminal groups ($-NH_2$ and $-OH$) on PAMAM dendrimers as well as a chromophore functionalized PAMAM dendrimer. Both $-NH_2$ terminated and dansyl-chromophore functionalized PAMAM G2−gold nanocomposites were prepared by the following procedures. Initially, $HAuCl_4$ and dendrimers were separately dissolved in water (PAMAM G2) or DMF. Both solutions were mixed and stirred with water or DMF to make the desired concentrations. The solutions were reduced by the addition of $NaBH_4$ under vigorous stirring for 3 h. The UV spectra of the dendrimer−gold nanocomposites illustrated the feature of gold nanoparticles with an absorption of ∼0.70 (with 1 mm cell) at the surface plasmon resonance (505 nm) for G2−NH_2−Au and 520 nm for dansylated G2−gold nanocomposites.

Dendrimer−gold nanocomposites containing an $-OH$ terminated PAMAM dendrimer G5 (G5−OH) as the host were also prepared. Two methods were used for this preparation. One method is by self-reduction; the other is an in situ intradendrimer exchange of Cu nanoparticles. In the first method, 16.8 μL of 3.59×10^{-3} M G5−OH was mixed with 1.5 mL of H_2O containing 0.28 mL of 9×10^{-3} M $HAuCl_4$. The mixture was stirred at room temperature under N_2. Upon mixing the two components, the color of the solution changed to purple-red. The UV−vis spectrum shows broad and red-shifted bands at 545 and 640 nm. This implies the metal nanoparticles are prone to aggregation[24] and the degree of metal particle aggregation is suggestively higher than that of the $-NH_2$ terminated G2−Au system. The second method for preparing G5−OH−Cu^{2+}−Au nanocomposites is the exchange of G5−OH−Cu nanocomposites. We utilized a similar procedure described in the literature.[25] Here, 66 μL of 3.78×10^{-3} M G5−OH was mixed with 80 μL of 0.1 M $Cu(NO_3)_2$ and then diluted to ∼5 mL by water. This mixture containing 32 Cu^{2+} ions per dendrimer was stirred at room temperature under N_2. After 20 min, a stiochiometric amount of freshly prepared 9.59×10^{-2} M $NaBH_4$ (85 μL) was added to the mixture. After 20 min, 0.69 mL of 9.083×10^{-3} M $HAuCl_4$ was added and diluted the mixture to 5 mL. The color of solution immediately changes to purple-red. The UV spectrum shows a new absorption feature of the SPR at 510 nm.

The characterization of the copper ion concentration [Cu^{2+}] in the G5−OH−Cu and G5−OH−Cu^{2+}−Au were carried out by a standardized spectrophotometric method.[26] This method is based on a quantitative extraction of copper and sodium diethyldithiocarbamate (Cu−$(DTC)_2$) complex in chloroform at pH 8−10. The absorbance at 436 nm is proportional to the amount of [Cu^{2+}] in the solution. In this experiment, 0.5 mL of the G5−OH−Cu or G5−OH−Cu^{2+}−Au was transferred into 50 mL flask and diluted with water. Then 10 mL of this solution was placed into 125 mL separation funnel and water (50 mL) was added. The pH was adjusted to 9.2 by the addition of 1:1 $NH_3 \cdot H_2O$ (2−4 drops of 0.04% Thymol Blue ethanol solution was used as a pH indicator). After mixing, 10 mL of 0.2% Na_2DTC was added to form the Cu−$(DTC)_2$ complex. This complex was extracted by 10 mL of $CHCl_3$. The UV spectrum was recorded and the absorbance at 436 nm was used for the quantization of [Cu^{2+}]. The same procedure was carried out for the standard preparation and standard curve measurements. The concentration of Cu^{2+} in the nanocomposites can be calculated by[26]

$$Cu^{2+}\ (mg/L) = \frac{m\frac{50}{10}}{0.5} \qquad (1)$$

SCHEME 1: Synthesis Pathway and the Structure of Dansylated G2

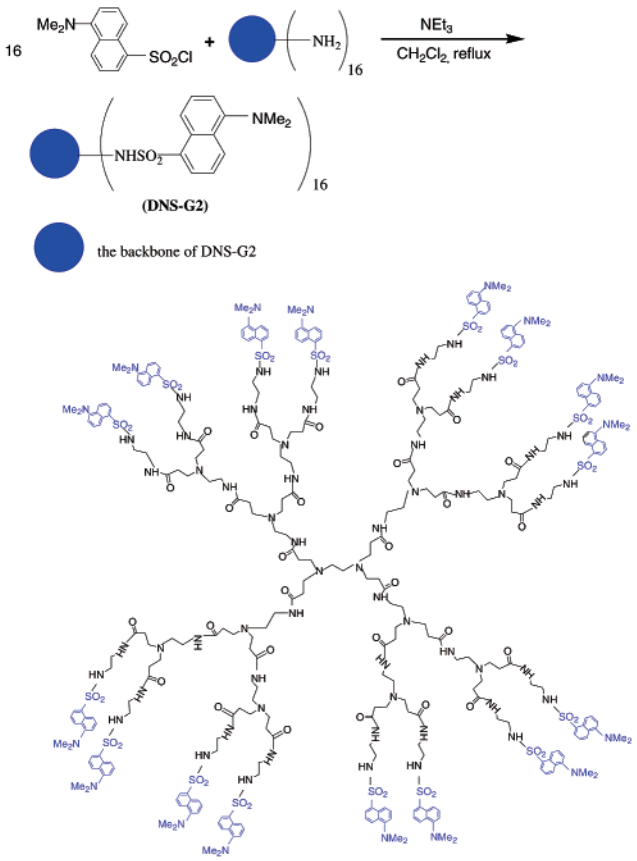

By this measurement, our results show that nearly half of the Cu^{2+} was reduced by a stiochiometric amount of $NaBH_4$ after 20 min and only 10% of Cu clusters remained after the replacement reaction. It is known that there is a balance between the reaction time and the stability of the nanocomposite system after the exchange reaction has taken place. In doing so, the relatively small amount of Cu cluster remaining was a good compromise for our preparation of the gold nanocomposite systems with this reaction time.

C. Synthesis of Dansylated PAMAM Dendrimer G2 (Scheme 1, DNS−G2). The synthetic procedure followed a similar protocol reported previously.[27−29] The crude product was purified by flash chromatography [silica gel, eluting with 1. $CHCl_3$, 2. $CHCl_3$:CH_3OH:Et_3N (10:0.5:0.1), 3. $CHCl_3$:CH_3OH:Et_3N (15:2:1)] to yield a yellow DNS−G2 (237.8 mg, yield 20%). TLC: $R_f = 0.50$ ($CHCl_3$:CH_3OH:Et_3N = 15:2:1). The ^1H NMR of the product in CD_2Cl_2 (400 MHz) is shown in Figure 1a. δ (ppm) 2.19−2.54 (m, 142H, 12×d−CH_2+2×a−CH_2+28×c−CH_2+28×b−CH_2), 2.70∼2.90 (m, 157H, 96H from 16 ×-N(CH_3)$_2$, and 64H from 16 ×-O_2SNHCH_2CH_2-NHCO-), 3.22 (br, s, 53H, e−CH_2), 7.11 (m, 29H, −CON*H*-), 7.41−7.54 (m, 48H; arom, H6+H3+H7), 8.13 (d, 16H, arom, H8), 8.25 (d, 16H, arom, H2), 8.47 (d, 16H, arom, H4). The ^{13}C NMR of DNS−G2 in CD_2Cl_2 is also displayed in Figure 1b. δ (ppm): 53.68, 53.94, 54.22 (*C*H_2 in dendrimer), 43.21 (SO_2NH*C*H_2-), 45.40 (−N(*C*H_3)$_2$), 115.4, 119.3, 123.4 (C_{dansyl}), 129.4, 130.0(*C*H_{dansyl}), 135.2, 152 (C_{dansyl}), 173.6 (*C*ONH). The proton numbers of the product calculated on the basis of the integration value 0.19 for one proton in ^1H NMR spectrum do coincide with the expected numbers in all regions where 16 dansyl chromophores were successfully attached on the dendrimer. The estimation of a complete conversion of the terminal

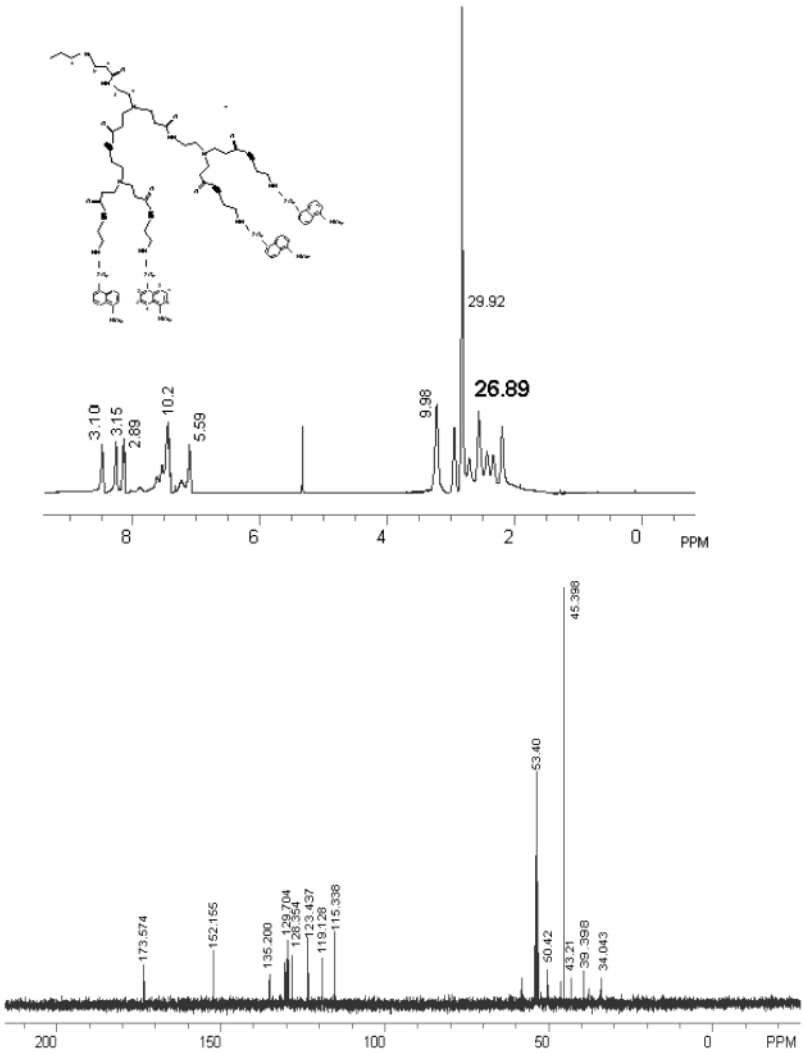

Figure 1. (a) ^{1}H NMR spectrum and (b) the ^{13}C spectrum of DNS−G2 in CD_2Cl_2

amine groups is further supported by ^{13}C because the signal of the methylene groups adjacent to the amino groups at 40 ppm which disappeared. A new peak at 43.21 ppm formed because of the methylene groups after dansylation (SO_2NHCH_2). Considering that the DNS−G2 was synthesized and purified by a method similar to dansylated poly(propylemine), these spectroscopic data for the DNS-G2 provided satisfactory characterization.

D. UV−vis Absorption and Fluorescence Measurements. The UV−vis absorption measurements were carried out using a Hewlett-Packard 8450 diode array spectrophotometer. Unless otherwise noted, a 1 mm cell was used to obtain the reported spectra. The UV−vis absorption was used as a way of standardizing the concentrations of gold nanoparticles in different samples at the transverse surface plasmon resonance. In this way, the comparison of the different gold nanostructured materials could be carried out. The steady-state emission from the gold rods, gold spheres, and dendrimer−gold nanocomposites were far too small to be observed with a common fluorescence spectrometer (RF-1501 spectrofluorophotometer). However, the fluorescence from the organic dye in DNS-G2-Au could be measured with different metal concentrations. The queching was observed in the presence of gold nanoparticles. The fluorescence decay of this system was also investigated by time-correlated single photon counting. Our time-correlated signle photon counting (TCSPC) set up consists of a Ti:sapphire laser, which has a repetition rate 82 MHz and a pulse width of 100 fs. Using the fundamental beam of 770 nm, the second harmonic of 385 nm was generated at the nonlinear crystal. The electronic software from *Picoquant* was used to analyze the fluorescence decay data.

E. Nonlinear Transmission Measurements. For the measurements of the nonlinear transmission effects in these novel gold nanostructures, we utilized a nonlinear transmission apparatus with similar parameters to those reported in the test beds of other interesting optical limiting materials.[19] A Nd:YAG laser operating at 532 nm (or 1064 nm) with pulse duration of ~6.5 ns and 10 Hz repetition rate was used. Most of the measurements were carried out at 532 nm because this allows direct excitation of the transverse absorption resonance in these gold nanostructures. The laser beam is focused with a f/25 lens in order to produce a beam spot of 37 μm in diameter. The sample is positioned in the focal plane. Two photodiode detetctors were used for the reference input and transmitted output intensities. The output photodiode is 30 cm away from the sample. A boxcar integrator and associated electronics is used to collect and analyze the transmitted light. Calibration curves were obtained for all experiments to correct the transmission values.

III. Results and Discussion

Gold Nanorods and Nanospheres

A. Absorption of Gold Nanorods and Nanospheres. Shown in Figure 2 are the absorption profiles for the gold nanospheres

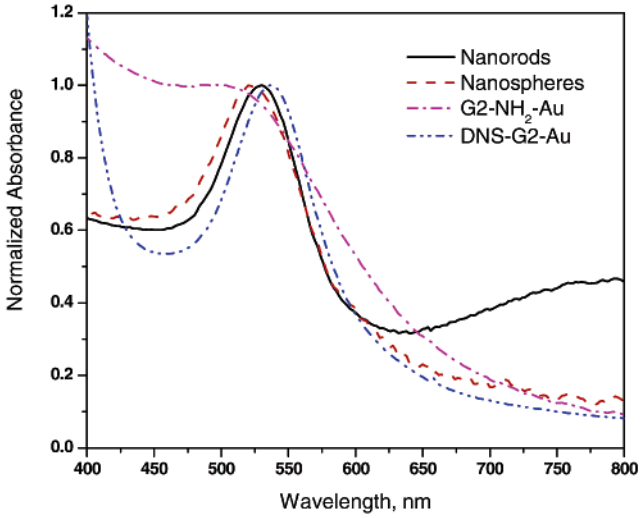

Figure 2. Absorption spectra of gold nanorods (aspect ratio 5.0), gold nanospheres, G2−NH_2−Au, and DNS−G2−Au (normalized at the maximum SPR).

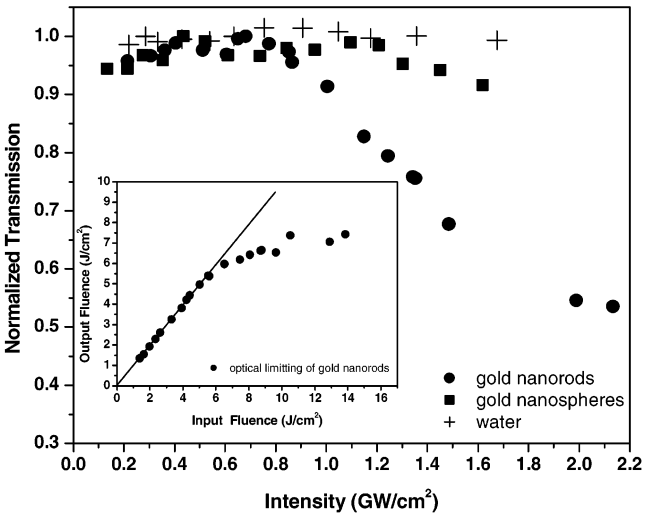

Figure 3. NLT of both the gold nanorods (●) and gold nanospheres (■) at 532 nm. Water (+) was used as a blank. The insert shows the optical limiting of the gold nanorods. The solid lines represents the constant transmission of 50%.

and nanorods used in this investigation. Here the diameter of gold nanospheres (35 nm) was estimated by transmission electron microscopy. The transverse (width) mode of the nanorods was ∼15 nm, and for this sample (aspect ratio 5.0), the longitudinal length is ∼75 nm. One easily identifies the very strong absorption near the transverse direction (520 nm) which is essential in characterizing the optical properties of these gold particles. In the case of the gold nanorods, another maximum is approximately 720 nm, which extends to the near-IR regions. This is important, as the strong IR light from the ns Nd:YAG laser could cause singificant absorption, even when the metal resonance is small. As it is often seen in the fabrication of nanorods by the electro-chemical technique,[11,14] the possibility that a small amount of nanospheres remaining after the electrochemical procedure is not excluded. Also, the distribution of aspect ratios of rods are not as narrow to suggest that there is a single rod length in the solution.[11,14a] However, from our measurements it is clear that the relatively small amount of spheres remaining in the nanorods solution does not obscure our nonlinear optical results.

B. Nonlinear Transmission (NLT) of Gold Nanorods and Nanospheres. Shown in Figure 3 is the NLT result for the gold nanospheres and nanorods. In these experiments, water was the solvent, and it was also used as a blank for the NLT measurements. There was no NLT effect for the blank water sample when measured at 532 nm with ∼6 ns pulses. What was surprising was that there was only a small NLT effect with ∼35 nm diameter gold nanospheres. Furthermore, as the input intensity reached levels close to 1.2 GW/cm^2, still only a small (but measurable) change in NLT was observed for the gold nanospheres. These results are in direct contrast to what was measured with the gold nanorods (Figure 3). The transmission dropped to 50% of its initial value over the same intensity range when comparable concentrations of metal particles were used. This result might suggest that the initial geometry of the metal particles is important in determining the nonlinear optical effects.

With ns pulse excitation, it has been found that intense direct excitation of gold nanostructures close to the SPR may result in a degradation of the geometry of the particles.[14] To probe this possibility; absorption spectra were recorded before and after the transmission measurements. For the case of nanorods, no detectable signs of depletion of plasmon bands at 520 and ∼800 nm were observed. After many reproducible experiments, the calculated two-photon absorption coefficient (β) was found to be 5.3 cm/GW for the gold nanorod sample. Shown in the insert of Figure 3 is the plot of fluence dependence (for optical limiting characterization) for the gold nanorods with aspect ratio 5.0. The optical limiting threshold was found to be 5.5 J/cm^2. This result is comparable to many other optical limiting materials reported in the literature.[18−20,23] For example, the EHO−OPPE an organic dye structure was reported to have a transmission decrease of 65% when input intensities as high as 0.6 GW/cm^2 were used.[19e] The Af-380 dye showed a threshold fluence of ∼2 J/cm^2 and a transmission loss of 60% for an input fluence increase up to 13 J/cm^2.[19f] Also, single-walled carbon nanotube suspensions have been reported showing a threshold fluence of ∼2 J/cm^2 and transmission decrease of 70%.[19g] However, the results of the nanorods do not meet the very high optical limiting standards of the important class of indium pthalocyanines or the novel metal clusters composed of both gold and silver.[20] Both of these systems have shown optical limiting thresholds as low as tens of microjoules.[20] However, the purpose of the present study is to determine the importance of the metal particle geometry on the nonlinear behavior rather than achieving a large magnitude of the NLT effect.

The principle goal behind the comparison of the NLO properties of gold nanospheres and nanorods is to probe the intrinsic difference in the optical excitations between the two nanostructures. As it has been calculated for the case of linear absorption and emission in metal nanostructures, local-field enhancement factors should play an important role in the electronic excitations of these architectures.[14,20] The linear absorption of the transverse resonance was the same for two solutions. In terms of the metal particles (spheres, rods, etc.), there have been a number of reports that have suggested mechanisms of the NLT in different metal topologies.[30−32] Mostafavi et al.[33] has investigated the size dependence and the mechanism of the NLT for gold particles with diameters 2.5, 9, and 15 nm. Interestingly, the optical limiting effects increased strongly with the size increase of the particles. In this case, the origin of the effect was assigned to the formation of strong light scattering centers due to the vaporization of the initial particles induced by the laser pulse.[34] It was suggested that the scattering centers are developed over a relatively slow time-scale (in comparison to intrinsic phenomena in gold particles)

SCHEME 2: Structure Illustration of Dendrimer−Gold Nanocomposites

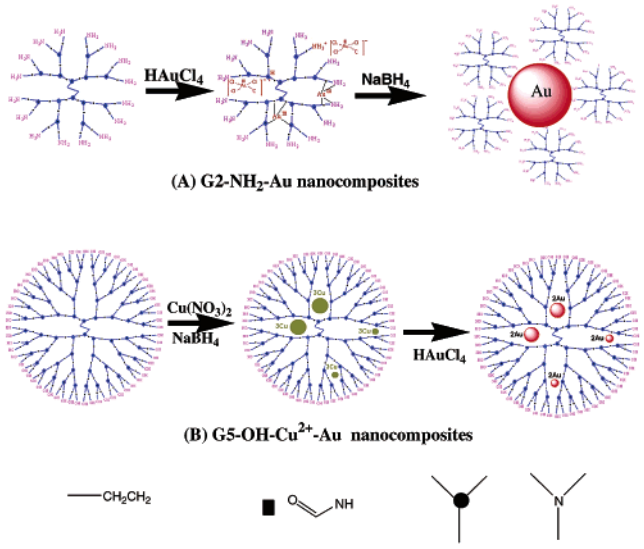

in a few nanoseconds and relax mostly reversibly with a partial degradation into small particles after repetitive pulses. This result is somewhat similar to our results with spheres in that the input fluencies are similar and the diameter of the second to largest nanoclustered sample in their series[33] is similar to the diameter of our spheres. However, their observation of changes in NLO properties after repeated pulses was not observed in our measurements for the rods or spheres. As stated above, the absorption profiles of the two systems were unchanged after our measurements and the NLT curves were reproducible.

Similar effects of nonlinear light scattering have already been reported with other metal nanostructures.[13,18,30−31,35−36] For example, Sun and co-workers[30,31] suggested that the optical limiting properties observed in silver nanoparticles could be associated with transient scattering processes that are attributed to photothermal processes. Dendrimer−silver nanocomposites were also shown to have interesting optical limiting effects which are associated with the strong light scattering processes that serve to diffuse the intensity of the input beam to very low (tolerable) levels.[18] The investigations of dendrimer−silver nanocomposites also suggested that the nonlinear transmission process is associated with scattering on relative large particles when sufficient input intensities are used. However, as in the case of the size-dependent optical limiting effects observed by Mostafavi et al.,[33] these processes are relatively slow in comparison to intrinsic optical excitations in the metal spheres and rods. It is thus apparent that at the intensity levels used in our measurements there is indeed a characteristic difference between the NLT effects (and mechanisms) associated with gold nanorods and gold nanospheres.

Another result which is related to the geometry of the nanorods and the process of infrared photochemical aggregation concerns the nonlinear transmission results of the rods at 1064 nm. For the aspect ratio 5.0 sample, we did observe a measurable nonlinear transmission effect at 1064 nm. However, the surface plasmon absorption of the aspect ratio 3.0 rods is far blue-shifted, and there was hardly any linear absorption at 1064 nm. It should be noted that if the mechanism of the NLT results that we observed from the rods only involved aggregation of metal particles then we surely should have observed the same effects with the spheres with different concentrations. It is thus apparent to us that the optical limiting properties of the rods most likely due to the strong light scattering processes.

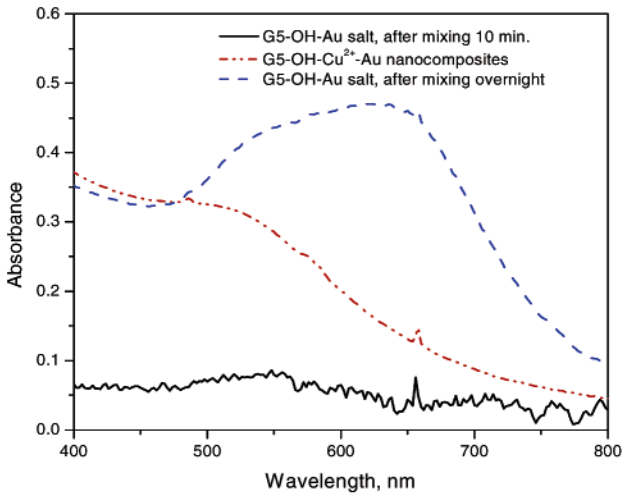

Figure 4. UV spectra of G5−OH−Cu^{2+}−Au and G5−OH−Au.

Dendrimer Gold Nanocomposites

C. Absorption of G2−NH_2−Au and DNS−G2−Au. Shown in Figure 2 is also a comparison UV spectra of G2−NH_2−Au and DNS−G2-Au. The shapes of the two profiles vary significantly but the absorption feature which corresponds to the surface plasmon resonance of Au nanoparticles is similar. The spectrum of G2−NH_2−Au shows a broad band with the maximum absorbance around 502 nm. The broader SPR reflects the dispersity of larger gold nanoparticles, which were stabilized by an interaction of the lone pair electrons of the amine with the surface of gold particles[10,37−38] (Scheme 2A). The stability of this G2−NH_2−Au (λ_{max} = 502 nm, A = 0.70) is weak. After 1 day of storage, the nanoparticles precipitated out of solution. Thus, great care had to be taken in order to efficiently carry out the experiments with fresh and reliable samples.

To analyze the effect of local field enhancement on the NLO properties of gold nanocomposites, a dansyl-chromophore functionalized G2 was used as a template. The UV spectrum of this nanocomposites shows a red-shifted and relative narrow SPR with the maximum absorbance at 536 nm (A = 0.7). In comparison with G2−NH_2−Au, the stability of these nanocomposites has been improved and can be stored for one month without any precipitation. One has to ask how the dendrimer structure itself changes after the functionalization of G2 by dansyl chromophores. Because dansyl chloride is a relatively small molecule that is attached to the (starlike) open structure of G2 PAMAM, it is reasonable to assume that the morphology of DNS-G2 would remain similar to the morphology of the G2−NH_2 system. This suggestion is of importance in the comparison of the NLT between G2−NH_2−Au and DNS−G2−Au.

D. Absorption of G5−OH−Cu^{2+}−Au and G5−OH−Au. Shown in Figure 4 is the absorption spectrum of G5−OH−Cu^{2+}−Au and G5−OH−Au. The UV spectrum of G5−OH−Cu^{2+}−Au prepared by a primary displacement reaction exhibited a surface plasmon band around 510 nm with a rather broad shoulder, indicating the formation of very small size of gold nanoparticles formed in the interior of G5−OH dendrimer[25] (Scheme 2B). It was also found that while mixing G5−OH with gold salt under N_2 gold nanoparticles are formed and the spectrum changed with time. After mixing for 10 min, the typical surface plasmon resonance of the gold nanoparticles was observed. However, with an elapsed time of a few hours, this surface plasmon absorption band is red-shifted and displays a broadened spectrum, suggesting the formation of larger aggregated gold nanoparticles. This formation may be attributed

to the reducing capacity of the terminal hydroxyl groups of the PAMAM dendrimer G5 as has been demonstrated in the "sugar ball" reduction of gold ions.[39,40] Because $AuCl_4^-$ forms a complex with interior tertiary amines of the PAMAM, the gold nanoparticles could partially be in the interior of G5−OH. Furthermore, as the −OH groups are oxidized to carbonyl groups,[40] the electron-rich carbonyl can interact with the surface of gold particles and stabilize the particles on the surface of dendrimer, as was also observed in the formation of "sugar ball-gold nanocomposites" system.[40]

E. Copper Ion Concentration Determination in the G5−OH−Cu Nanocomposite. As described in the Experimental Section, the synthesis of G5−OH−Cu^{2+}−Au was carried out by intradendrimer exchange method. The result of quantitative determinations of the number of Cu^{2+} extracted into the PAMAM dendrimer G6−OH and G4−OH suggests that each dendrimer G5−OH can load 32 Cu^{2+}.[25] The chemical reduction of Cu^{2+}-loaded G5−OH dendrimer with $NaBH_4$ gives intradendrimer Cu clusters.[25] However, in our experiment, the initially formed golden brown Cu cluster solution gradually changes to blue with time, even in the excess of $NaBH_4$ and under N_2. Therefore, we investigated how much Cu^{2+} would remain in the G5−OH−Cu as a function of the reaction time. Because the Cu cluster may be oxidized by O_2, the experimental procedure should be carried out with great care of possible O_2 contamination. In fact, the pH of the mixture will increase after the addition of excess of $NaBH_4$. For example, with further addition (3X) of $NaBH_4$, the pH 7.5 solution of G5−OH−Cu^{2+} reached pH 9.5. We also found that the self-reduction (mixing of G5−OH with Au^{3+}) can easily occur under basic conditions. Therefore, to avoid pH changes, a stoichiometric amount of $NaBH_4$ was added to reduce Cu^{2+} (pH = 7.2∼7.5). The remaining Cu^{2+} was detected by the absorption method. The results indicate that nearly half Cu cluster is formed after 20 min reduction.

By using the intradendrimer exchange method, stable and small (∼2 nm) amounts of Au nanoparticles can be prepared by the Cu exchange reaction

$$2Au^{3+} + 3Cu^0 = 2Au^0 + 3Cu^{2+} \qquad (2)$$

As mentioned above, it is impossible to reduce all Cu^{2+} into Cu clusters. However, to have all Cu clusters exchanged as gold nanoparticles, we added the stoichiometric amount of $HAuCl_4$ into the G5−OH (Cu−Cu^{2+}) solution. After the replacement reaction was completed (after 20 min) under N_2, the sample was examined for Cu^{2+} traces. The results indicate that about 10% Cu cluster remains. Indeed, in our NLT measurement, we excited these nanocomposites at the SPR of gold nanopartilces (532 nm); therefore, the possible NLT from this 10% Cu cluster would be insignificant.

F. Nonlinear Transmission of G2−NH_2−Au, G5−OH−Au. The use of G2 and G5 dendrimers as templates for gold nanoparticles would allow us to examine how the dendrimers morphology affects the NLO properties. Figure 5 shows the NLT of the G2−NH_2−Au. The solvents (DMF and water) have no NLT effect. The observed change in NLT for the G2−NH_2−Au is ∼70%. This change is very strong at the intensities used in these experiments (see above discussion concerning the experimental parameters). If we take 1.4 GW/cm^2 as our point of reference, we can see that a 70% change in NLT of G2−NH_2−Au has already occurred, whereas the gold nanorods have only 30% change in NLT. This would suggest that the dendrimer metal nanocomposite has a significant enhancement in the NLT effect at high input powers as compared to the gold nanorods

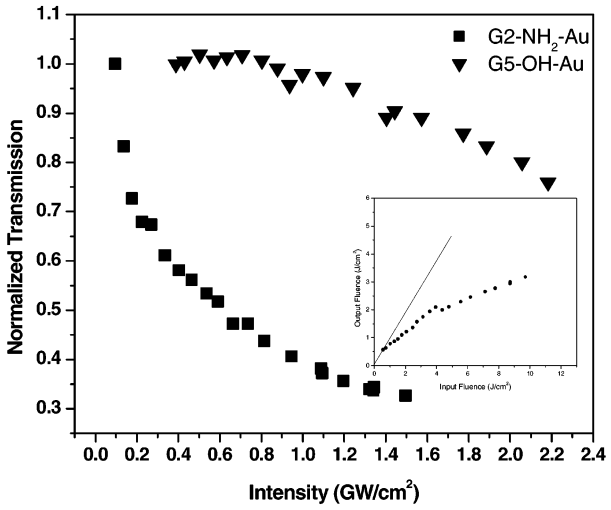

Figure 5. Nonlinear transmission result of G2−NH_2−Au and G5−OH−Au. The insert is the optical limiting of G2−NH_2−Au.

(see above comparisons). This effect has been observed in other hybrids materials[41,42] and dendrimer−silver nanocomposites.[18] The insert of Figure 5 shows the optical limiting of G2−NH_2−Au. The nanocomposite system has a threshold that is found to be ∼4 J/cm^2. To examine whether the particular dendrimers play a role in the magnitude of NLT of gold nanoparticles, the spherical G5−OH was chosen to prepare gold nanocomposites and the NLT of these nanocomposites was examined. In the case of G5−OH−Au, a 25% change in NLT was obtained (Figure 5) when all the experimental parameters were the same for all of the systems studied. This result suggests that the magnitude of NLT of gold nanoparticles does depend on its templates.

G. Interaction between Dansylated G2 and Gold Nanoparticles. To explain the subsequent NLO results of DNS-G2-Au and compare these results with those obtained from the same moropholgy of G2−NH_2−Au, it is important to first understand the interactions among dansyl chromophores attached to G2 and the interactions of dansyl units with gold nanoparticles. Investigations of fluorescence lifetimes can provide insight into the interaction of dansyl chromophores and the results would help us to understand the NLO properties. Thus, the time-correlated single photon counting was used to characterize the fluorescence lifetimes of DNS−G2. For comparison, dansyl chloride was chosen as a reference compound. The fluorescence decays of 8.48×10^{-8} M DNS−G2 and 1.36×10^{-6} M dansyl chloride (DNS−Cl) (Figure 6) could be satisfactory fit by a two-exponential function given as

$$I(t) = A_1 e^{-(\tau_1/t)} + A_2 e^{-(\tau_2/t)} \qquad (3)$$

where A_1 and A_2 are constants proportional to the magnitude of the contribution of the components and τ_1 and τ_2 are decay times. These parameters were found to be $A_1 = 1081$, $\tau_1 = 0.445$ ns, $A_2 = 1506$, and $\tau_2 = 6.78$ ns for DNS-G2 and $A_1 = 1852$, $\tau_1 = 0.303$ ns, $A_2 = 2249$, and $\tau_2 = 2.93$ ns for DNS−Cl. The significant difference in the lifetimes indicates that there are strong interactions among the dansyl groups attached to the dendrimer. Further measurements were performed with the dendrimer metal nanocomposite system functionalized with the dansyl chromophore. In this case, a strong decrease in the fluorescence lifetime was observed consistent with strong interactions of the metal particles with the chromophores attached to the PAMAM dendrimer.

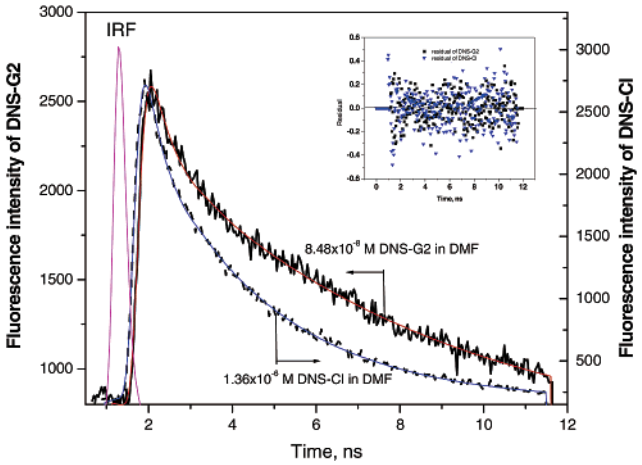

Figure 6. Time-resolved fluorescence in 8.48×10^{-8} M dansylated G2 and 1.36×10^{-6} M dansyl chloride upon excitation at 385 nm, emission at 510 nm. The traces are fitted with two-exponential function. The insert shows the residuals of experimental data and the solid lines are the fitted curves.

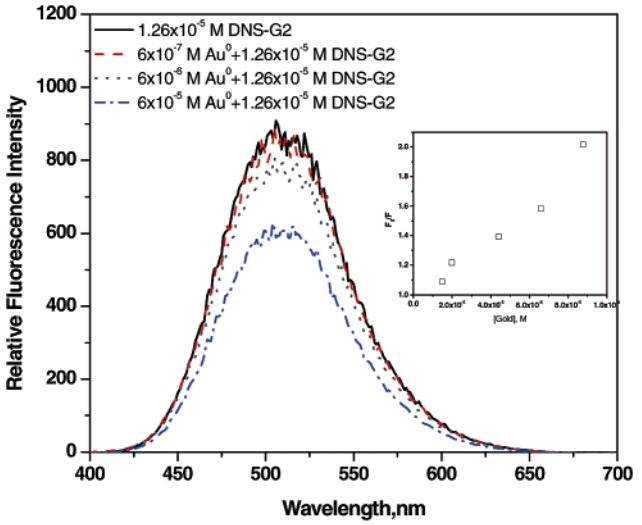

Figure 7. Fluorescence quenching of DNS−G2 by various concentrations of gold nanoparticles. The insert shows the fluorescence quenching efficiency with the concentration increasing of gold nanoparticles.

The interactions of chromophores with the metal may also affect the nonlinear transmission of the metal nanocomposites. Steady-state fluorescence measurements were carried out for the investigation of these interactions. Shown in Figure 7 is the fluorescence spectra of 1.26×10^{-5} M DNS−G2 at various concentrations of gold nanoparticles. The quenching efficiency, defined as fluorescence intensity ratio (F_0/F) in the absence and in the presence of metal, is plotted against metal concentration (Figure 7 insert). It can be seen from this figure that the quenching increases with increasing concentration of gold nanoparticles. There are three mechanisms concerning the effect of metal surface on a fluorophore: one is the quenching of fluorophore via energy transfer from dye to metal, another is an increase in the fluorophore emission by increased excitation field, and the last is an increase of fluorophore emission (low quantum yield) by increased radiative decay rate.[43] Because emission and energy transfer are competitive processes, the efficiency depends on the relative values of the emission and energy transfer. Less has been reported on the effect of the metal surface on collisional quenching. In our case, it is highly plausible that the quenching results from the excited-state interactions via nonradiative energy transfer from the dye to metal.[44] These strong interactions are also important to the details of the NLT of DNS-G2-Au.

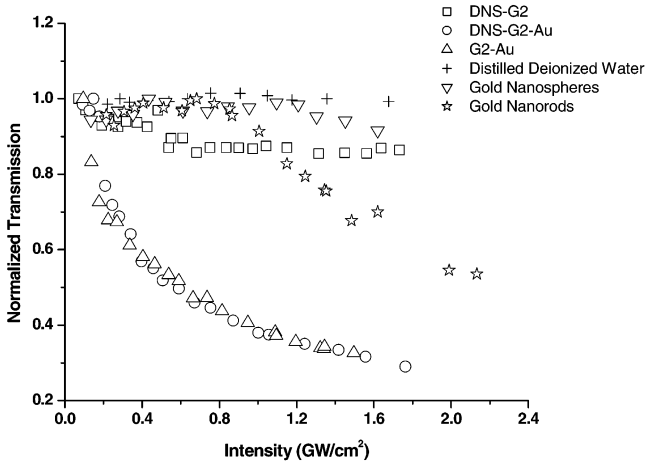

Figure 8. Comparison of NLT effects of gold rods, spheres, G2−Au, DNS−G2, and DNS−G2−Au.

H. NLT Comparison of Gold Nanocomposites. Figure 8 shows the NLT comparison of gold nanorods, spheres, G2−NH_2−Au, DNS−G2, and DNS−G2−Au. At 532 nm, the DNS−G2 has only a weak NLT effect. However, the DNS−G2−Au shows a significant NLT effect. As mentioned above, there are strong interactions between dansyl units and metal. Also, the long lifetime of DNS−G2 may suggest it is possible that the excited-state absorption is enhanced due to the excitation of the SPR of gold nanoparticles, as suggested by Qu and the co-workers.[20] Thus, we would expect to observe a larger NLT effect for the chromophore functionalized dendrimer metal nanocomposite in comparison to the G2−NH_2−Au. However, the results of the two nanocomposites are comparable when metal concentrations are similar. This implies that the dominate NLT effect is due to the characteristics of the gold nanoparticles and that the NLT attributed to excited state absorption is relatively week for the case of the chromophore functionalized dendrimer system.

IV. Conclusion

We have characterized the linear and nonlinear optical properties of several metal nanoparticle topologies. Our finding is that the geometries of metal particles play an important role in the NLO effect. The TPA value for the nanorods is significantly larger than that observed for the gold nanospheres. Also, we found that the dendrimer−metal morphology affects the NLO properties. The observation of the NLO response from G5−OH−Au, and not from G5−OH−Cu^{2+}−Au illustrates how the metal particle's size affects the observed NLT. The results of fluorescence quenching measurements indicate that there is a strong interaction between dansyl chromophores attached to the dendrimer and the metal nanoparticles. These results, along with the previous G4−Ag dendrimer nanocomposites reported in the literature,[18] further demonstrate that the mechanism of NLO effect is mainly due to light scattering of the metal nanoparticle assisted by increased aggregation of the particles in some of the templates. This study provides an insight into how certain geometries of metal nanoparticles and dendrimer nanocomposite topologies may influence the NLO processes.

Acknowledgment. This work was funded by Army Research Office, and the Air force Office of Scientific Research, and the National Science Foundation. We are very gratefully to Professor

M. El-Sayed and M. Mohamed for providing the nanorods and nanospheres samples.

References and Notes

(1) Ng, M. K.; Lee, D. C.; Yu, L. P.; *J. Am. Chem. Soc*., **2002**, 124, 11862.
(2) Rowan, S. J.; Stoddart, J. F. *J. Am. Chem. Soc.* **2000**, *122*, 164.
(3) Wang, Y. Z.; Sun, R. G.; Meghdadi. F.; Leising, G.; Swager, T. M.; Epstein, A. J. *Synth. Met.* **1999**, *102* (1−3), 889.
(4) Tomalia, D.; Baker, H.; Dewald, J.; Hall, M.; Kallos, G.; Martin, S.; Roeck, J.; Ryder, J. Smith, P. *Macromolecules* **1986**, *19*, 2466.
(5) Pastoriza-Santos, I. Liz-Marzán, L. M. *Langmuir* **1999**, *15*, 948.
(6) Kowshik, M.; Deshmukh, N.; Vogel, W.; Urban, J.; Kulkarni, S. K.; Paknikar, K. M. *Biotechnol. Bioeng.* **2002**, *78* (5), 583.
(7) Thilakan, P.; Kazi, Z. I.; Egawa, T. *Appl. Surf. Sci.* **2002**, *191* (1−4), 196.
(8) Zhao, M.; Crooks, R. M. *Angew. Chem., Int. Ed. Engl.* **1999**, *38*, 364.
(9) Esumi, K.; Torigoe, K. *Prog. Colloid Polym. Sci.* **2001**, *117*, 80.
(10) Gröhn, F.; Bauer, B. J.; Akpalu, Y. A.; Jackson, C. L. Amis, E. J. *Macromolecules* **2000**, *33*, 6042.
(11) Yu, Y.-Y.; Chang, S.-S.; Lee, C.-L. Wang, C. R. C. *J. Phys. Chem. B* **1997**, *101*, 6661.
(12) Li, Y.; El-Sayed, M. A. *J. Phys. Chem. B* **2001**, *105*, 8938.
(13) Sun, Y.-P.; Riggs, J. E.; Henbest, K. B.; Martin, R. B. *J. Nonlinear Opt. Phys. Mater.* **2000**, *9* (4), 481.
(14) (a) Chang, S.-S.; Shih, C.-W.; Chen, C.-D.; Lai, W.-C. Wang, C. R. C. *Langmuir* **1999**, *15*, 701. (b) Mohamed, M. B.; Volkov, V.; Link, S.; El-Sayed, M. A. *Chem. Phys. Lett.* **2000**, *317*, 517. (c). Varnavski, O.; Mohamed, M.; El-Sayed, M.; Goodson, T. *Phys. Rev. Lett.* (submitted).
(15) Kreibig, U.; Vollmer, M. *Optical properties of metal cluster*; Springer: Berlin, 1995.
(16) Shipway, A. N.; Katz, E. Willner, I. *Chem. Phys. Chem.* **2000**, *1*, 18.
(17) Sonnichsen, C.; Franzl, T.; Wilk, T.; von Plessen, G.; Feldmann, J.; Wilson, O.; Mulvaney, P. *Phys. Rev. Lett.* **2002**, *88* (7), 077402.
(18) Ispasoiu, R. G.; Balogh, L.; Varnavski, O. P.; Tomalia, D. A.; Goodson, T., III. *J. Am. Chem. Soc.* **2000**, *122*, 11005.
(19) (a) Sun, N.; Wang, Y.; Song, Y.; Guo, Z.; Dai, L. Zhu, D. *Chem. Phys. Lett.* **2001**, *344*, 277. (b) Nalwa, H. S.; Shirk J. S. In *Phthalocyanines: Properties and Applications*; Leznoff, C. C., Lever, A. B. P., Eds.; VCH Publishers: New York, 1996; pp 4, 79. (c) Xia, T. J.; Hagan, D. J.; Dogariu, A.; Said, A. A.; Van Stryland, E. W. *Appl. Opt*. **1997**, *36*, 4110. (d) Zhang, H.; Zelmon, D. E.; Deng, L.; Liu, H. K.; Boon, K. T. *J. Am. Chem. Soc.* **2001**, *123*, 11300. (e) He, G. S.; Weder, C.; Smith, P.; Prasad, P. *IEEE J. Quantum Electron.* **1998**, *34*, 2279. (f) Joshi, M. P.; Swiatkiewicz, J.; Xu, F.; Prasad, P.; Reinhardt, B. A.; Kannan, R. *Opt. Lett*. **1998**, *23*, 1742. (g) Mishra, S. R.; Rawat, H. S.; Mehendale, S. C.; Rustagi, K. C.; Sood, A. K.; Bandyopadhyay, R.; Govindaraj, A.; Rao, C. N. R. *Chem. Phys. Lett*. **2000**, *317*, 510.
(20) Qu, S.; Song, Y.; Du, C.; Wang, Y.; Gao, Y.; Liu, S.; Li, Y.; Zhu, D. *Opt. Comm.* **2001**, *196*, 317.
(21) Sun, Y.-P. Riggs, J. E. *Int. Rev. Phys. Chem.* **1999**, *18*, 43.
(22) Kneipp Katrin, *Single Mol.* **2001**, *2* (4), 291.
(23) Sun, N.; Guo, Z.-X.; Dai, L.; Zhu, D.; Wang, Y. Song, Y. *Chem. Phys. Lett.* **2002**, *356*, 175.
(24) Zheng, J.; Stevenson, M. S.; Hikida, R. S.; Van Patten, P. G. *J. Phys. Chem. B* **2002**, *106* (6), 1252.
(25) Zhao, M. Crooks, R. M. *Chem. Mater.* **1999**, *11*, 3379 and reference cited therein.
(26) *Standard methods for the examination* Cu^{2+} *in water and waster water (in Chinese)*; Technical Standard Publisher: Beijing, 1982; p 49.
(27) Vögtle, F.; Gestermann, S.; Kauffmann, C.; Ceroni, P.; Vicinelli, V. Balazani, V. *J. Am. Chem. Soc.* **2000**, *122*, 10398.
(28) Vögtle, F.; Gestermann, S.; Kauffmann, C.; Ceroni, P.; Vicinelli, V.; Cola, L. D. Balazani, V. *J. Am. Chem. Soc.* **1999**, *121*, 12161.
(29) Balzani, V.; Ceroni, P.; Gestermann, S.; Gorka, M.; Kauffmann, C. Vögtle, F. *J. Chem. Soc., Dalton Trans.* **2000**, *21*, 3765.
(30) Sun, Y.; Riggs, J. E.; Henbest, K. B.; Martin, R. *J Nonlinear Opt. Phys. Mater*. **2000**, *9*, 481.
(31) Riggs, J. E.; Sun, Y.-P. *J. Phys. Chem. A* **1999**, *103*, 485.
(32) Bigot, J.-Y.; Halté, V.; Merle, J.-C. Daunois, A. *Chem. Phys.* **2000**, *251*, 181.
(33) François, L.; Mostafavi, M.; Belloni, J.; Delouis, J. F.; Delaire, J. A.; Feneyrous, P. *J. Phys. Chem. B* **2000**, *104*, 6133.
(34) François, L.; Mostafavi, M.; Belloni, J.; Delaire, J. A. *Phys. Chem. Chem. Phys.* **2001**, *3*, 4965.
(35) Shen, Y.-C.; Tang, Z.; Gui, M.; Cheng, J.; Wang, X.; Lu, Z. *Chem. Lett.* **2000**, 1140.
(36) Pileni, M. P. *Nanostructured Maerials*; Shalaev, V. M., Moskovits, M., Eds.; American Chemical Society: Washington, DC, 1997.
(37) Garcia, M. E.; Baker, L. A.; Crooks, R. M. *Anal. Chem.* **1999**, *71*, 256.
(38) Esumi, K.; Suzuki, A.; Yamahira, A.; Torigoe, K. *Langmuir* **2000**, *16*, 2604.
(39) Esumi, K.; Hosoya, T.; Suzuki, A. Torigoe, K. *J. Colloid Interface Sci.* **2000**, *226*, 346.
(40) Esumi, K.; Hosoya, T.; Suzuki, A.; Torigoe, K. *Langmuir* **2000**, *16*, 2978.
(41) Qu, S.; Chen, Y.; Wang, Y.; Song, Y.; Liu, S.; Zhao, X.; Wang, D. *Mater. Lett.* **2001**, *51*, 534.
(42) Perry, J. W.; Mansour, K.; Lee, I.-Y. S.; Wu, X.-L.; Bedworth, P. V.; Chen, C.-T.; Ng, D.; Marder, S. R.; Miles, P.; Wada, T.; Tian, M. Sasabe, H. *Science* **1996**, *273*, 1533.
(43) Lakowicz, J. R. *Anal. Biochem.* **2001**, *298*, 1.
(44) Chance, R. R.; Prock, A. S. R. *Adv. Chem. Phys.* **1978**, *37*, 1.